Separation Science and Technology
Publication details, including instructions for authors and subscription information:
http://www.informaworld.com/smpp/title~content=t713708471

Analysis and Prediction of Sieving Curves for Ultrafiltration Membranes: A Universal Correlation?

Alan S. Michaels[a]
[a] DEPARTMENT OF CHEMICAL ENGINEERING, STANFORD UNIVERSITY STANFORD, CALIFORNIA

To cite this Article Michaels, Alan S.(1980) 'Analysis and Prediction of Sieving Curves for Ultrafiltration Membranes: A Universal Correlation?', Separation Science and Technology, 15: 6, 1305 — 1322
To link to this Article: DOI: 10.1080/01496398008068507
URL: http://dx.doi.org/10.1080/01496398008068507

SEPARATION SCIENCE AND TECHNOLOGY, 15(6), pp. 1305–1322, 1980

Analysis and Prediction of Sieving Curves for Ultrafiltration Membranes: A Universal Correlation?

ALAN S. MICHAELS

DEPARTMENT OF CHEMICAL ENGINEERING
STANFORD UNIVERSITY
STANFORD, CALIFORNIA 94305

Abstract

Sieving curves [variations in sieving coefficient (θ) with Einstein-Stokes radius (a) of the permeating macromolecule] of a number of synthetic ultrafiltration membranes, and of a variety of mammalian glomerular membranes studied *in vivo*, conform surprisingly closely to a log-normal-probability relationship between θ and a which allows determination of the complete sieving curve from experimental measurement of only two sieving coefficients for two macrosolutes of differing ESR. Even more striking is the finding that, for all membranes examined, the value of a corresponding to $\theta = 0.5$ (the inflection point in the sieving curve) varies only between 17 and 34 Å, and geometric standard deviation about the mean macrosolute radius (σ_a), which is inversely related to the "sharpness" of the sieving curve, lies between 1.2 and 1.7. It is concluded that not only is the log-probability correlation a reasonable and convenient means for interpreting and predicting membrane sieving data, but that most natural and synthetic ultrafiltration membranes have very closely related matrix morphologies.

In 1976, Green et al. (*1*) reported data on the sieving coefficients of two hemodialysis membranes [Cuprophan and Rhone-Poulenc's RP 69 poly(acrylonitrile) membrane] when operated as ultrafilters, and found that the sieving coefficients for the two membranes varied with the Einstein-Stokes radius (ESR) of the permeating macrosolutes in a manner which yielded straight (and parallel) lines on normal probability coordinates. While their mathematical representation of the consequence of this correlation was in error, and their inferences about the relations between

a sieving curve and a membrane pore-size distribution incorrect, their observations seemed to us to be sufficiently provocative to merit closer scrutiny as a basis for correlation of the sieving (rejection) characteristics of a variety of natural and synthetic ultrafiltration membranes.

There is a large body of data in the literature describing the macrosolute sieving behavior of commercially-available polymeric ultrafiltration and dialysis membranes, and of mammalian glomerular membranes. The most commonly employed "probe" solutes for these measurements are monodisperse purified proteins, and polydisperse, linear, water-soluble macromolecules exemplified by the dextrans and their derivatives, poly(vinyl pyrrolidone) and poly(ethylene glycol). Dextran has been extensively employed in human and animal kidney-clearance studies because of its nontoxicity, stability, availability in widely differing molecular weight ranges, and relative ease of analysis.

The ESR is the traditional parameter used to characterize a macrosolute in ultrafiltration studies; it is the "apparent equivalent spherical radius" of the macromolecule as computed from the measured diffusivity of the molecule in free solution by using the Stokes-Einstein equation:

$$D = kT/6\pi\eta a$$

where D is the measured diffusion coefficient, η is the solvent viscosity, and a is the ESR. The ESR has unequivocal physical meaning only for a rigid, spherical particle in a fluid continuum, and its significance for asymmetric, solvated, free-draining, or compliant-chain macromolecules is ambiguous.

For polydisperse polymer mixtures, gel-permeation chromatography has become well established as a technique for determining molecular size and size-distribution. For aqueous-phase GPC, it is customary to calibrate the chromatographic column with a series of monodisperse proteins of known ESR, and to ascribe to the chromatographic fractions eluted from the column the same ESR as that of a protein displaced at the corresponding elution-volume. ESR values determined by GPC are, therefore, empirical characterization parameters related in some complex way to "effective molecular size." For a homologous series of polymer molecules, however, the ESRs determined by GPC undoubtedly correlate monotonically with the "true" molecular radii important in determining ultrafiltrative rejection, but to equate such a parameter to a genuine molecular dimension would be ill-advised.

The sieving coefficient, θ, of an ultrafiltration membrane for a particular solute is the fraction of that solute present in the solution upstream of the membrane which is delivered in the ultrafiltrate. This coefficient (or its complement, the rejection coefficient $R = 1 - \theta$) varies between zero

and unity with changing solute "molecular size" to yield a characteristic S-shaped "sieving curve." The similarity of appearance of these sieving curves to cumulative-particle-size-distribution curves for particulate solids has undoubtedly been responsible for suggesting a probabilistic approach to correlating membrane rejection data.

The use of the normal probability (Gaussian distribution) function to correlate sieving coefficients with ESR, as proposed and tested by Green et al., is *functionally* inadmissible, since this distribution function is finite and symmetrical about all positive *and negative* values of its argument. Since negative values of molecular radius (or pore radius) are impossible, a more acceptable and reasonable correlation-basis is the *log-normal* distribution function; the cumulative probability function is then given by

$$\Phi = 1 - \text{erf}\,(z) \tag{1}$$

where

$$\text{erf}\,(z) = \frac{1}{\sqrt{2\pi}} \int_{-\infty}^{u} \exp\,(-y^2/2)\,dy \tag{2}$$

and

$$z = \frac{\log\,(x/\bar{x})}{\log\,\sigma_g} \tag{3}$$

where x is the value of a particular population in the distribution, $\bar{x}$ is the geometric mean, and σ_g is the geometric standard deviation about the mean.

If the sieving coefficient θ correlates with Einstein-Stokes radius a via the log-normal probability function, then the analytical relationship between θ and a will be

$$\theta = 1 - \text{erf}\,(\tau) \tag{4}$$

where

$$\tau = \frac{\log\,(a/\bar{a})}{\log\,\sigma_a} \tag{5}$$

and a is the ESR of the permeating molecule, $\bar{a}$ is the ESR of the "mean" molecule (for which $\theta = 0.5$), and σ_a is the geometric standard deviation about the mean ESR.

On log-probability coordinates, Eqs. (4) and (5) linearize in the form

$$F(\theta) = A + B[\log a] \tag{6}$$

whence, if $F(0.5) = 0$,

$$F(\theta) = \frac{\log a}{\log \sigma_a} - \frac{\log \bar{a}}{\log \sigma_a} = \tau \tag{7}$$

Thus, when $\log(a/\bar{a})/\log\sigma_a = 1.0$ (or $a/\bar{a} = \sigma_a$), $\theta = 0.159$; hence σ_a can be determined from the ratio of a at $\theta = 0.159$ (or $\theta = 0.841$) and $\bar{a}$ at $\theta = 0.5$. Sieving curves which linearize on log-probability coordinates, therefore, are completely defined by *two characteristic constants*: (1) the "mean ESR," $\bar{a}$, for which $\theta = 0.5$; and (2) the geometric standard deviation, σ_a. Evidence of the validity of this basis for correlating the sieving coefficients as functions of solute molecular weight for ultrafiltration membranes has recently been provided by Cooper (*2*) for a polydisperse neutral dextran and a series of asymmetric hollow-fiber membranes. Since the ESR is expected to be a simple power function of molecular weight for a homologous series of macromolecules, a log-normal relation between sieving coefficient and ESR of the form of Eq. (7) is expected for this system.

We have reexamined a number of recent publications reporting experimentally determined values of the ultrafiltration sieving coefficients (and their molecular-size dependency) for the glomerular membranes of the kidneys of the rat, the dog, and man, wherein the probe macrosolutes studied have included neutral dextrans, dextran sulfate, diethylaminoethyl dextran, Ficoll (an epichlorhydrin crosslinked polymer of sucrose), and poly(vinyl pyrrolidone) for the purpose of testing the applicability of this log-normal probability correlation. In addition, published sieving-coefficient data for several synthetic polymeric membranes, as determined with dextrans, PVP, and other probe macrosolutes of known ESR, have been similarly evaluated. The results of this exercise are summarized below.

GROUP I: NORMAL MAMMALIAN GLOMERULI; UNCHARGED MACROSOLUTES

Table 1 and Fig. 1 present sieving coefficient data for the normal

TABLE 1

Sieving Curves for Normal Mammalian

Curve no.	Species	Source	Probe solute	18	20	22	24	26
1	Rat	Chang (*9*)	Dextran	0.99	0.96	0.92	0.82	0.69
2	Rat	Chang (*3*)	Dextran	0.99	0.99	0.97	0.92	0.83
3	Rat	Bohrer (*4*)	Dextran	1.00	0.97	0.87	0.73	0.60
4	Rat	Bohrer (*5*)	Ficoll	0.96	0.96	0.93	0.86	0.74
5	Dog	Lambert (*6*)	PVP	—	—	0.68	0.50	0.39
6	Dog	Verniory (*7*)	PVP	—	—	0.82	0.74	0.63
7	Man	Myers (*8*)	Dextran	—	0.97	0.90	0.80	0.74

(Wistar) rat glomerulus with respect to neutral dextrans [Chang (*3*), Bohrer (*4*)] and Ficoll [Bohrer (*5*)]; for the normal dog glomerulus to polydisperse poly(vinyl pyrrolidone) [Lambert (*6*), Verniory (*7*)]; and for the normal human glomerulus to dextrans [Myers (*8*)]. As will be seen from Fig. 1, the log-normal probability relationship against ESR is closely obeyed for all the data sets. Linear regression analysis of the data has been performed [recognizing that $F(\theta)$ is the inverse error function]; the appropriate mean values of $\bar{a}$ and σ_a are tabulated in Table 1 for each data set, along with the coefficient of correlation, r^2.

The results are significant on at least three counts:

(1) The coefficients of correlation for the seven independent data sets vary between a minimum of ~ 0.97 and a maximum of > 0.99. This, of course, indicates that the log-normal-probability relationship between sieving coefficient and macrosolute ESR is an extraordinarily accurate representation of the sieving curves for these membranes.

(2) The "mean macrosolute ESRs," $\bar{a}$, for the glomeruli of the three species studied—corresponding to a θ of 0.50—differ surprisingly little. In man, the value appears to be slightly over 30 Å; for the rat, perhaps 28 to 29 Å; and for the dog, around 25 Å.

(3) The geometric standard deviation about the mean (σ_a) for all three species is very nearly identical, lying between 1.2 and 1.3. This quantity is a direct measure of the "sharpness" of the rejection spectrum of the membrane, indicating that, functionally, glomerular membranes of these three mammalian species must be morphologically almost identical.

Another rather interesting and provocative observation is the finding that the rat glomerular sieving curve with respect to polydisperse Ficoll

Glomeruli and Neutral Macrosolutes

θ vs a, Einstein-Stokes radius (Å)										
28	30	32	34	36	38	40	42	$\bar{a}$ (Å)	σ_a	r^2
0.56	0.44	0.33	0.23	0.15	0.08	0.05	0.03	28.9	1.22	0.999
0.69	0.55	0.42	0.30	0.19	0.11	0.06	0.03	30.4	1.20	0.987
0.45	0.32	0.22	0.15	0.09	0.045	0.02	—	27.4	1.20	0.996
0.60	0.44	0.28	0.16	0.09	0.04	0.02	—	28.0	1.20	0.969
0.28	0.23	0.14	0.09	0.06	—	—	—	24.5	1.29	0.995
0.50	0.40	0.30	0.22	0.15	0.10	—	—	26.1	1.30	0.998
0.62	0.55	0.44	0.34	0.26	0.20	0.15	—	30.3	1.30	0.986

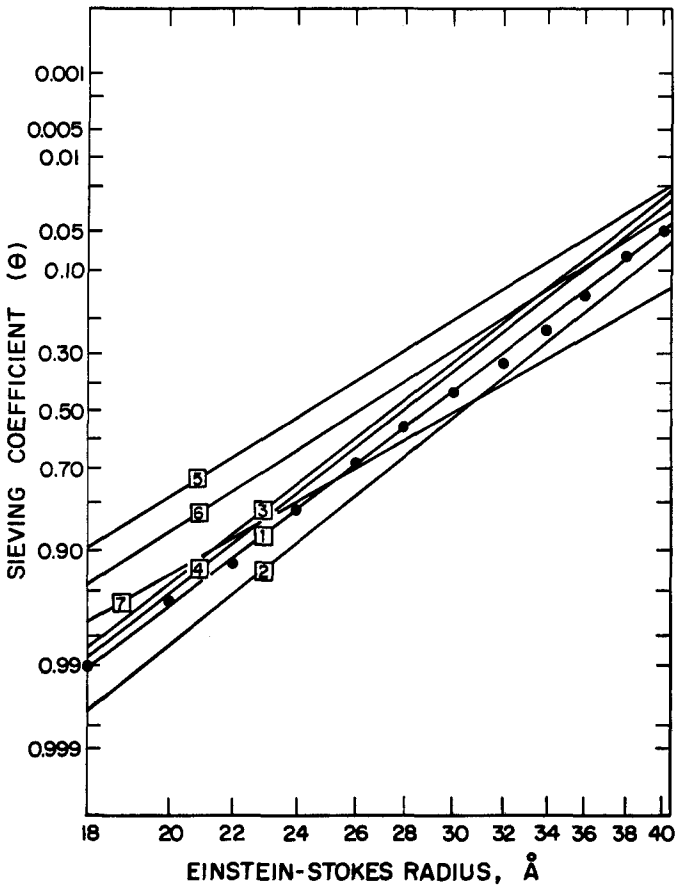

FIG. 1. Sieving curves for normal mammalian glomeruli and uncharged macrosolutes. (Numbers on lines correspond to entries in Table 1; points on graph are experimental data points corresponding to Line 1.)

is substantially identical to that measured with polydisperse neutral dextran. Inasmuch as it is known that the conformation of Ficoll molecules in solution is substantially different from (more spheroidal than) that of dextran, this result might not have been expected. Since, however, the putative ESRs of both polymeric species were assigned on the basis of their elution times from the same precalibrated Sephadex gel-permeation chromatographic column, one is tempted to postulate that the molecular conformational parameters which govern gel-permeation dynamics within hydrogels such as Sephadex are very closely related to those which

govern macrosolute transport through ultrafiltration membranes. A comparison of the apparent molecular dimensions of dextran and Ficoll species displaying the same apparent ESR by GPC, using some other "size"-measuring technique such as laser-Doppler autocorrelation spectroscopy, is likely to clarify this important question.

GROUP II: NORMAL VS NEPHROTIC RAT KIDNEYS; NEUTRAL VS IONOGENIC MACROSOLUTES

In the absence of electrostatic interactions between a permeating macromolecule and an ultrafiltration membrane [a condition which should obtain if either membrane or macromolecule (or both) were uncharged], and if specific van der Waals force-interactions between membrane and macrosolute are not significant, then the principal determinant of the sieving coefficient should be the size and conformation of the penetrating molecule, and the morphology of the membrane matrix. This indeed seems to be borne out with "normal" glomeruli and neutral macromolecules. Since, however, the glomerular membrane is known to be normally negatively charged, and since pathological changes in the membrane are frequently accompanied by changes in membrane microstructure and charge density, use of this log-normal-probability-correlation to characterize the response of normal and pathological glomeruli to neutral, anionic, and cationic macromolecules was expected to be informative.

Data are presented for polydisperse sodium dextran sulfate [Chang (*9. 10*), Bohrer (*4*)], and for polydisperse diethylaminoethyl dextran [Bohrer (*11*)] with normal rat glomeruli, and also for neutral and charged dextrans with rat glomeruli displaying pathologies induced by chemical treatments known to cause irreversible glomerulonephrosis. Results are summarized in Table 2 and Fig. 2.

For data-sets 8, 9, and 10, which constitute sieving curves for ionically charged dextrans through the normal rat glomerulus, the log-probability correlation continues to describe the experimental data quite accurately, with coefficients of correlation in the range ~ 0.99. It is noteworthy that, for dextran sulfate, the "mean" ESR, $\bar{a}$, is depressed to ~ 20 Å from nearly 30 Å for neutral dextran, whereas $\bar{a}$ for DEAE dextran is elevated to about 34 Å. Such a result is qualitatively consistent with electrostatic retardation of penetration of the negatively charged macromolecule through a negatively charged membrane, and enhancement of penetration of a positively charged macromolecule. The concomitant observation that σ_a values for charged solutes are also elevated above those observed for neutral dextran (1.25 to 1.29 vs ~ 1.20) lends credibility to this hypothesis: σ_a is a measure of the "sharpness-of-cutoff" of the membrane (for $\sigma_a =$

TABLE 2

Sieving Curves for Charged Macrosolutes and

Curve no.	Condition	Source	Probe solute	18	20	22	24	26
8	Normal	Chang (*3*)	Dextran sulfate	0.74	0.58	0.42	0.29	0.19
9	Normal	Bohrer (*4*)	Dextran sulfate	0.56	0.35	0.19	0.11	0.06
10	Normal	Bohrer (*11*)	DEAE dextran	1.00	0.99	0.97	0.93	0.87
11	A-II[a]	Bohrer (*4*)	Dextran	1.00	0.99	0.95	0.85	0.74
12	A-II	Bohrer (*4*)	Dextran sulfate	0.74	0.55	0.37	0.25	0.16
13	NSN[b]	Bohrer (*11*)	Dextran	0.90	0.86	0.81	0.73	0.63
14	NSN	Bohrer (*11*)	Dextran sulfate	0.90	0.86	0.81	0.75	0.66
15	NSN	Bohrer (*11*)	DEAE dextran	0.83	0.78	0.72	0.66	0.58
16	PAN[c]	Bohrer (*4*)	Dextran	0.88	0.82	0.69	0.56	0.43
17	PAN	Bohrer (*4*)	Dextran sulfate	—	0.97	0.90	0.80	0.74

[a]Treatment with angiotension II. Causes irreversible transglomerular leakage of albumin
[b]Induced nephrotoxic serum nephritis.
[c]Treatment with puromycin aminonucleoside. Causes lipoid nephrosis and disorganiza-

1.0, a membrane would display a step change in sieving coefficient from 0.0 to 1.0 for a macrosolute of ESR = $\bar{a}$). An increase in σ_a indicates a reduction of membrane separation capacity on a basis of macrosolute size, and it is logical that electrostatic interactions should (if repulsive) tend to cause preferential retardation of transport of small molecules or (if attractive) cause relatively enhanced transport of large ones.

If, however, the log-normal probability correlation for the sieving coefficient were to have some fundamental physical significance for describing the macrosolute rejection behavior of *neutral* membranes toward *neutral* macrosolutes, it seems unlikely that such a correlation would be equally applicable to membrane/macrosolute systems wherein electrostatic or electrokinetic phenomena are also involved in the sieving process. Accordingly, we do not believe there is any rational basis for ascribing a physicochemical explanation to the correlation; nonetheless, the correlation is an extremely good approximation to the experimental observations.

Examination of the sieving coefficient/ESR data (Table 2, Fig. 2, Entries 11 to 17) for rat glomeruli subjected to chemical or biochemical insults known to induce irreversible changes in glomerular membrane-structure characteristic of glomerular nephroses (such changes resulting in partial collapse of the membrane-matrix and loss of much of the normal negative charge-functionality of the membrane) shows that the log-probability correlation continues to be an accurate representation of the sieving

Normal and Pathologic Rat Glomeruli

θ vs a, Einstein-Stokes radius (Å)										
28	30	32	34	36	38	40	42	$\bar{a}$ (Å)	σ_a	r^2
0.13	0.09	0.05	0.03	0.015	0.01	—	—	21.0	1.29	0.998
0.03	0.02	0.01	0.01	—	—	—	—	18.1	1.28	0.989
0.80	0.74	0.66	0.56	0.44	0.32	0.20	0.11	34.0	1.25	0.987
0.59	0.46	0.32	0.22	0.14	0.075	0.04	0.02	19.3	1.19	0.998
0.10	0.06	0.04	0.02	0.01	—	—	—	20.7	1.25	0.992
0.50	0.38	0.28	0.20	0.14	0.09	0.05	0.025	27.1	1.29	0.980
0.56	0.46	0.39	0.31	0.24	0.18	0.11	0.05	28.5	1.35	0.973
0.49	0.39	0.31	0.22	0.15	0.09	0.05	0.03	30.3	1.27	0.986
0.30	0.21	0.14	0.07	0.05	0.02	0.01	0.01	26.2	1.34	0.960
0.62	0.55	0.44	0.34	0.26	0.20	0.15	—	24.5	1.26	0.996

and other plasma proteins.

tion of the glomerular epithelium.

curves (r^2 values between 0.96 and 0.99). For neutral dextran, these membrane changes (Entries 11, 13, and 16) are accompanied by a reduction in $\bar{a}$ and usually an increase in σ_a; this is an anticipated consequence of a shrinkage-induced reduction in "mean pore size" and a corresponding widening of the "pore size distribution." For dextran sulfate these same membrane changes (Entries 12, 14, and 17) lead to an *increase* in $\bar{a}$; this observation is consistent with a decline in negative-charge-density within the membrane, with consequent loss in Donnan-exclusion of polyanions. For DEAE dextran (a cationic polymer), the trend with glomerular membrane-damage (Entry 15) is toward reduction in $\bar{a}$, a result again consistent with loss in electrostatic augmentation of polycation transport with loss of membrane negative charge. It is thus apparent that the log-probability correlation, and the two characteristic parameters $\bar{a}$ and σ_a which are derived from that correlation, can facilitate interpretation of sieving curves in terms of membrane matrix structural features.

GROUP III: SYNTHETIC ULTRAFILTRATION MEMBRANES

The sieving coefficient data obtained by Green et al. (*1*) for Cuprophan and the Rhone-Poulenc AN 69 dialysis membrane (an asymmetric, microporous polyacrylonitrile structure) are reported in Table 3. These data also linearize quite well on log-probability coordinates (see Fig. 3),

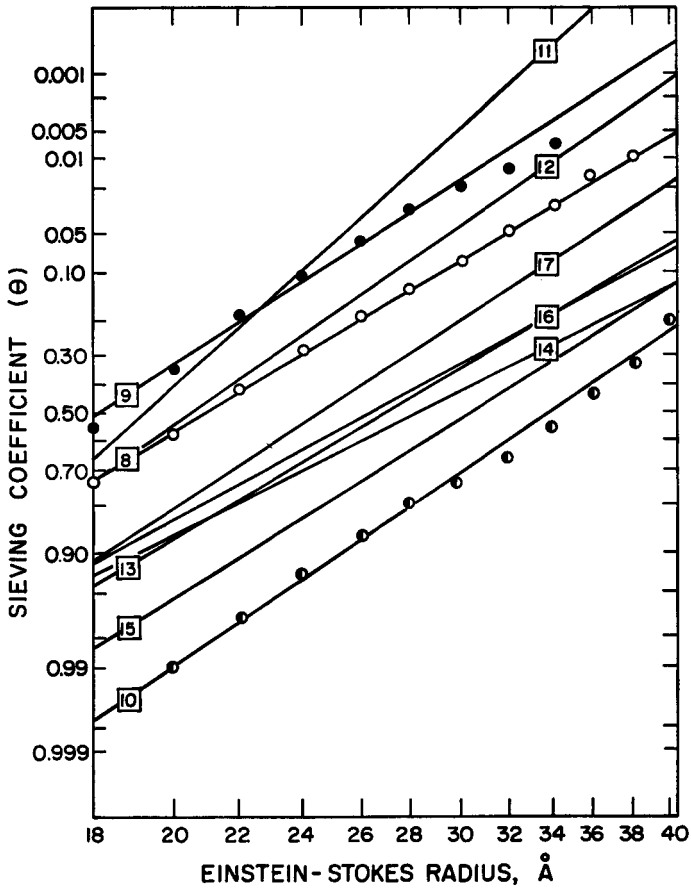

FIG. 2. Sieving curves for normal and pathologic rat glomeruli, and uncharged and ionogenic dextrans. (Numbers on lines correspond to entries in Table 2; points on graph are experimental data points corresponding to Lines 8, 9, and 10.)

TABLE 3

Correction of Sieving Coefficients Reported by DuBois (*12*) for Transport of Polydisperse PVP through XM-50 Membranes

Operating pressure (cm H_2O)	ESR (Å)	J_v (cm/sec) $\times 10^5$	Calculated mass transfer coefficient,[a] k (cm/sec $\times 10^5$)	exp (J_v/R)	Measured sieving coefficient, θ_a	True sieving coefficient, θ
5	16	0.5	7.6	1.07	0.96	0.96
	20		6.6	1.08	0.86	0.85
	24		5.8	1.09	0.79	0.78
	28		5.2	1.10	0.66	0.64
	32		4.8	1.11	0.46	0.43
	36		4.4	1.12	0.24	0.22
	40		4.1	1.13	0.12	0.11
	44		3.9	1.14	0.06	0.05
	48		3.7	1.14	0.03	0.03
30	16	3.0	7.6	1.48	0.82	0.75
	20		6.6	1.58	0.59	0.48
	24		5.8	1.68	0.45	0.33
	28		5.2	1.78	0.38	0.26
	32		4.8	1.87	0.20	0.12
	36		4.4	1.98	0.16	0.09
	40		4.1	2.08	0.06	0.03
	44		3.9	2.16	0.04	0.02
	48		3.7	2.25	0.02	0.01

[a]Via method of Smith et al. (*13*).

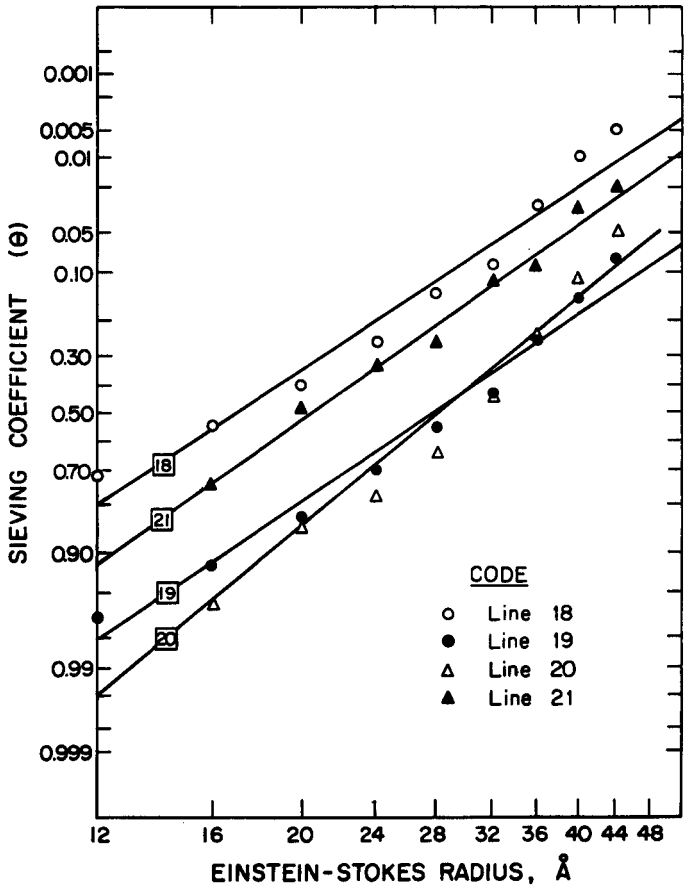

FIG. 3. Sieving curves for synthetic ultrafiltration membranes. (Numbers on lines correspond to entries in Table 3.)

yielding correlation coefficients between 0.97 and 0.98. The slopes of the lines for these two membranes are nearly identical ($\sigma_a \cong 1.5$), although the values of $\bar{a}$ (corresponding to $\theta = 0.5$) differ substantially.

DuBois et al. (*12*) measured sieving coefficients, using a polydisperse polyvinyl pyrrolidone, for several synthetic, asymmetric ultrafiltration membranes (Diaflo) manufactured by Amicon Corp. Their experiments were conducted in a stirred, batch ultrafiltration cell which the authors assumed provided sufficient agitation to eliminate concentration polarization; our computations, however, indicate that polarization may have been significant in most of their determinations. Their sieving data obtained with XM-50 membranes at low pressures were amenable to correction for polarization using the mass-transfer-coefficient correlation for stirred cells developed by Smith et al. (*13*) and Colton et al. (*14*), and the estimated trans-membrane water flux (J_v), to compute the Sherwood Number (J_v/k) for each PVP molecular radius. The results of these computations are summarized in Table 4 where the measured and "true" sieving coefficients are tabulated as functions of ESR for two different operating pressures. As expected, the polarization correction is rather small for the low-pressure (lower flux) run, but is significant for the higher-flux run. As shown in Table 3 and Fig. 3, the corrected sieving curves obey the log-probability correlation quite well (r^2 between 0.97 and 0.99). The observed decrease in slope (or increase in σ_a) and $\bar{a}$ with increasing J_v is consistent with the Kedem-Spiegler theory of coupled solute/solvent transport through ultrafiltration and hyperfiltration membranes: With increasing water-flux, the relative diffusive contribution of solute-leakage to total solute transport (most marked for smaller solute molecules) is reduced, rendering the sieving curve flatter, and lowering the value of $\bar{a}$ corresponding to $\theta = 0.5$.

Finally, we have taken the sieving data reported by Cooper et al. (*2*) for polydisperse dextran through Amicon PM-5 and PM-10 hollow fiber ultrafiltration membranes (which relate sieving coefficients to dextran molecular weight), computed the ESR values for the various molecular weight dextrans using the correlation proposal by Granath (*15*, *16*) based on dextran diffusion measurements:

$$a = 0.33(M)^{0.463} \tag{8}$$

and retabulated and replotted their data with θ a function of a. As shown in Table 3, the log-probability correlation is a very accurate representation of the function ($r^2 \geqq 0.99$) for both membranes. Interestingly, the PM-5 (nominal 5000 MW cutoff) and PM-10 (nominal 10,000 MW cutoff) display nearly identical values of $\bar{a}$, but the former has a smaller σ_a than the latter. Thus the PM-5 membrane may be characterized as having a

TABLE 4
Sieving Curves for

Curve no.	Membrane	Equipment	ΔP (cm H_2O)	Membrane water permeability [mL/(min) (cm^2) (cm H_2O)]	Probe solute	Source	12
18	Cuprophan	Dialysis cell	2,100	2.8×10^{-6}	Various species	Green (*1*)	0.72
19	RP 69	Dialysis cell	1,033	3.7×10^{-5}	Various species	Green (*1*)	0.97
20	Amicon XM-50	Stirred UF cell	5	6×10^{-5}	PVP	DuBois (*12*)[a]	
21	Amicon XM-50	Stirred UF cell	30	6×10^{-5}	PVP	DuBois (*12*)[a]	
22	Amicon PM-10	Hollow fiber module	?	$\sim 10^{-4}$	Neutral dextran	Cooper (*2*)	
23	Amicon PM-5	Hollow fiber module	?	$\sim 10^{-4}$	Neutral dextran	Cooper (*2*)	

[a] Corrected via method of Smith et al. (*13*).

"narrower pore-size distribution" than does the PM-10, although the "mean pore size" of the two membranes is nearly the same. These observations emphasize the inadequacy of a *single* parameter (such as the "molecular weight cutoff") as a useful descriptor of the sieving characteristics of an ultrafiltration membrane.

GENERAL OBSERVATIONS

Perhaps the most surprising and astonishing observation to be drawn from the foregoing analysis is not the apparent universality of the log-probability correlation to describe ultrafiltration membrane sieving curves (which is surely operationally convenient, but of doubtful theoretical significance), but the extraordinary similarity of all the sieving curves. Consider that the data analyzed include (1) normal and diseased glomerular membranes of three mammalian species; (2) synthetic, substantially homogeneous, dialysis membranes; and (3) synthetic, polymeric, asymmetric ultrafiltration membranes, the range of $\bar{a}$ values falls between 17 and 34 Å, and of σ_a only between 1.2 and 1.7. This suggests that virtually all membrane ultrafilters, irrespective of their origin, are quite similar in their microstructure. On balance, glomerular membranes display significantly narrower pore-size distributions (σ_a values lie between 1.2 and 1.3)

Synthetic Membranes

θ vs a, Einstein-Stokes radius (Å)											
16	20	24	28	32	36	40	44	48	$\bar{a}$ (Å)	σ_a	r^2
0.55	0.40	0.26	0.14	0.09	0.03	0.01	—	—	17.0	1.50	0.968
0.92	0.83	0.70	0.55	0.43	0.25	0.15	0.08	—	27.7	1.49	0.978
(0.96)	(0.86)	(0.79)	(0.66)	(0.46)	(0.24)	(0.12)	(0.06)	(0.03)			
0.96	0.85	0.78	0.64	0.43	0.22	0.11	0.05	0.02	28.2	1.33	0.974
(0.82)	(0.59)	(0.45)	(0.38)	(0.20)	(0.16)	(0.06)	(0.04)	(0.02)			
0.75	0.48	0.33	0.26	0.12	0.09	0.03	0.02	0.01	20.5	1.45	0.987
MW		7,000	11,000	18,000	28,000	43,000					
ESR, Å		19.8	24.5	30.8	37.8	46.1			18.3	1.66	0.988
θ		0.47	0.26	0.14	0.07	0.04					
MW		3,200	4,800	7,500	12,000	18,000	28,000				
ESR, Å		13.8	16.7	20.5	25.5	30.8	37.8		17.6	1.49	0.997
θ		0.74	0.53	0.38	0.16	0.08	0.03				

than do synthetic ultrafilters (σ_a values between 1.3 and 1.7), although their "mean pore size" (represented by $\bar{a}$) may span as broad a range as those of synthetic polymeric membranes.

Reexamination of Eqs. (4) and (5) indicates that the "universal" sieving coefficient vs solute ESR correlation can be reduced to dimensionless form by defining θ in terms of a "reduced ESR" ($a/\bar{a}$) and the (already dimensionless) geometric standard deviation about the mean ESR, σ_a. By plotting θ against $a/\bar{a}$ for various parametric values of σ_a, a family of generalized sieving curves can be generated upon which experimentally determined sieving coefficients for a specific membrane can be located to obtain complete sieving curves for that membrane. Such a generalized correlation is presented in Fig. 4. If, for a given membrane, one has determined the sieving coefficients for two macrosolutes of differing ESR, the ratio of the values of a corresponding to those two sieving coefficients uniquely determines the valu of σ_a, and thus also of $\bar{a}$, for that membrane. For example, if a membrane displays a sieving coefficient of 0.75 for a solute of ESR = 21 Å, and 0.35 for a solute of ESR = 30 Å, these points fall on the line for $\sigma_a \cong 1.4$, and lead to a value of $\bar{a} \cong 26$ Å. Thus Fig. 4 can be used to estimate the entire sieving curve for a membrane from a knowledge of only two sieving coefficients for two different macrosolutes, without recourse to algebraic manipulation of Eqs. (4)–(7).

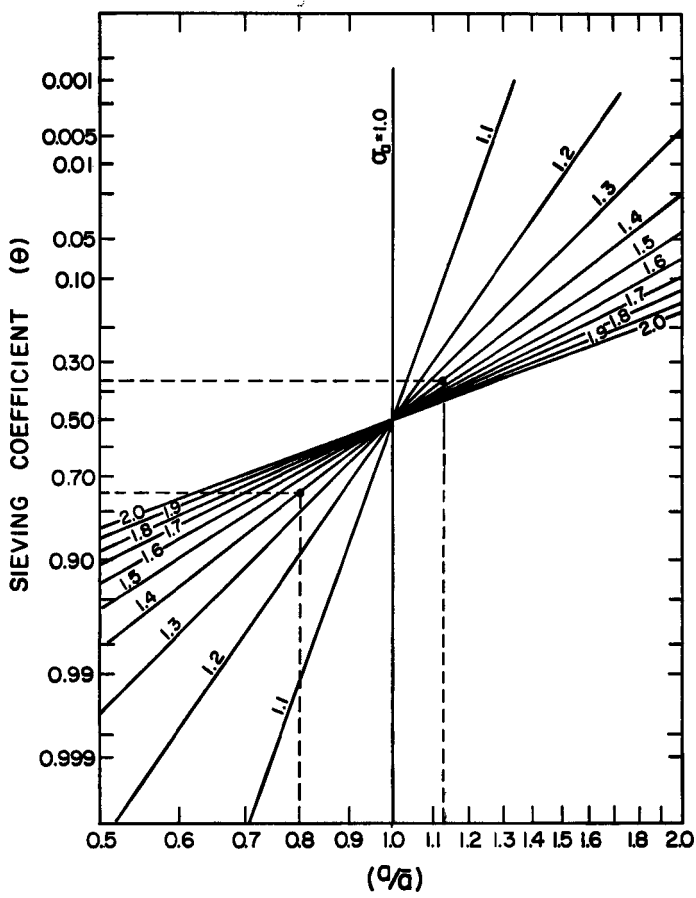

FIG. 4. Generalized sieving curves for membranes of varying σ_a values. (Dotted lines illustrate means for determining entire sieving curve from two arbitrary data-points: e.g., $\theta = 0.35$ when $a = 30$ Å; $\theta = 0.75$ when $a = 21$ Å. In this case, the sieving curve lies on the line corresponding to $\sigma_a = 1.4$.)

It is concluded that the log-normal probability function is a generally accurate means for describing sieving curves for ultrafiltration membranes, and can be used quite reliably to construct a complete sieving curve for a given membrane from only two experimental sieving-coefficient values for two differing solutes of known ESR. Of particular note is the observation that a wide variety of synthetic and biological membranes falls within a quite narrow range of apparent mean pore size and size-distribution, suggesting that all such membranes have very similar morphologies. Further experimental tests of this correlation, via experi-

mental determination of sieving coefficients of a number of synthetic ultrafiltration membranes toward a variety of macrosolutes of known Einstein-Stokes radii, are currently in progress and will be the subject of a subsequent paper.

SYMBOLS

a	Einstein-Stokes radius, Å, 10^{-8} cm
$\bar{a}$	geometric mean ESR, Å, 10^{-8} cm
D	diffusivity, cm^2/sec
k	Boltzman constant, ergs/(molecule) (°K)
M	molecular weight of a dextran fraction
T	absolute temperature, °K
x	arbitrary value of a population of a distribution
$\bar{x}$	geometric mean value of the distribution
z	generalized argument of the error function, dimensionless
η	solvent viscosity, dyn-sec/cm^2
θ	sieving coefficient, dimensionless
$F(\theta)$	inverse error function of θ, dimensionless
σ_g	geometric standard deviation of x, dimensionless
σ_a	geometric standard deviation of a, dimensionless
τ	argument of the error function in terms of a, $\bar{a}$, and σ_a, dimensionless

Acknowledgments

This study was conducted under the auspices and support of the Office of Water Research and Technology, U.S. Department of the Interior, and the Satellite Dialysis Center of San Jose, California.

REFERENCES

1. D. M. Green, G. D. Antwiler, J. W. Mancrief, J. F. Decherd, and R. P. Popovich, *Trans. Am. Soc. Artif. Intern. Organs*, *22*, 627 (1976).
2. A. R. Cooper and D. S. Van Derveer, *Sep. Sci. Technol.*, *14*, 551 (1979).
3. R. L. S. Chang, I. K. Ueki, J. L. Troy, W. M. Deen, C. R. Robertson, and B. M. Brenner, *Biophys. J.*, *15*, 887 (1975).
4. M. P. Bohrer, W. M. Deen, C. R. Robertson, and B. M. Brenner, *Am. J. Physiol.*, *223*, F13 (1977).
5. M. P. Bohrer, W. M. Deen, C. R. Robertson, and J. L. Troy, "Influence of Molecular Configuration on the Passage of Macromolecules Across the Glomerular Capillary Wall," To Be Published in *J. Gen. Physiol.* (1980).
6. P. P. Lambert, A. Verniory, J. P. Gassee, and P. Ficheroulle, *Kidney Int.*, *2*, 131 (1972).

7. A. Verniory, R. DuBois, P. Decoudt, J. P. Gassee, and P. P. Lambert, *J. Gen. Physiol.*, *62*, 489 (1973).
8. B. D. Myers, F. Chui, M. Hilberman, and A. S. Michaels, "Transtubular Leakage of Glomerular Filtrate in Human Acute Renal Failure," *Am. J. Physiol.*, *273* (4), F319–F325 (1979).
9. R. L. S. Chang. W. M. Deen, C. R. Robertson, and B. M. Brenner, *Kidney Int.*, *8*, 212 (1975).
10. R. L. S. Chang, W. M. Deen, C. R. Robertson, C. M. Bennett, R. J. Glassock, and B. M. Brenner, *J. Clin. Invest.*, *57*, 1272 (1976).
11. M. P. Bohrer, C. Baylis, H. D. Humes, R. J. Glassock, C. R. Robertson, and B. M. Brenner, *Ibid.*, *61*, 72 (1978).
12. R. DuBois and E. Stoupel, *Biophys. J.*, *16*, 1427 (1976).
13. K. A. Smith, C. K. Colton, E. W. Merrill, and L. B. Evans, "Convective Transport in a Batch Dialyzer: Determination of True Membrane Permeability from a Single Measurement," *Chem. Eng. Prog. Symp. Ser.*, *84* (64), 59 (1968).
14. C. K. Colton, S. Friedman, D. E. Wilson, and R. S. Lee, *J. Clin. Invest.*, *51*, 2472 (1972).
15. K. Granath, *J. Colloid Sci.*, *13*, 308 (1958).
16. K. Granath and B. Kvist, *J. Chromatogr.*, *28*, 69 (1967).

Received by editor November 19, 1979